Vehicle System Dynamics: International Journal of Vehicle Mechanics and Mobility

Publication details, including instructions for authors and subscription information:
http://www.tandfonline.com/loi/nvsd20

Stability analysis of a nonlinear vehicle model in plane motion using the concept of Lyapunov exponents

Sobhan Sadri [a] & Christine Wu [a]

[a] Department of Mechanical and Manufacturing Engineering , University of Manitoba , Winnipeg , Manitoba , Canada

Published online: 04 Mar 2013.

To cite this article: Sobhan Sadri & Christine Wu (2013): Stability analysis of a nonlinear vehicle model in plane motion using the concept of Lyapunov exponents, Vehicle System Dynamics: International Journal of Vehicle Mechanics and Mobility, 51:6, 906-924

To link to this article: http://dx.doi.org/10.1080/00423114.2013.771785

Vehicle System Dynamics, 2013
Vol. 51, No. 6, 906–924, http://dx.doi.org/10.1080/00423114.2013.771785

Taylor & Francis
Taylor & Francis Group

Stability analysis of a nonlinear vehicle model in plane motion using the concept of Lyapunov exponents

Sobhan Sadri and Christine Wu*

Department of Mechanical and Manufacturing Engineering, University of Manitoba, Winnipeg, Manitoba, Canada

(*Received 8 August 2012; final version received 18 January 2013*)

For the first time, this paper investigates the application of the concept of Lyapunov exponents to the stability analysis of the nonlinear vehicle model in plane motion with two degrees of freedom. The nonlinearity of the model comes from the third-order polynomial expression between the lateral forces on the tyres and the tyre slip angles. Comprehensive studies on both system and structural stability analyses of the vehicle model are presented. The system stability analysis includes the stability, lateral stability region, and effects of driving conditions on the lateral stability region of the vehicle model in the state space. In the structural stability analysis, the ranges of driving conditions in which the stability of the vehicle model is guaranteed are given. Moreover, through examples, the largest Lyapunov exponent is suggested as an indicator of the convergence rate in which the disturbed vehicle model returns to its stable fixed point.

Keywords: stability analysis; 2-DOF vehicle model; nonlinear tyre model; concept of Lyapunov exponents; stability region

1. Introduction

Vehicle safety as one important issue in transportation systems is followed by the road traffic safety administrations around the world. According to National Highway Traffic Safety Administration of USA (NHTSA), rollover is one of the most dangerous accidents that jeopardises vehicle occupant safety [1]. One type of rollovers is known as on-road untripped rollovers, which happen due to vehicle manoeuvring. Although this type of rollover is a small part of all rollovers (less than 10%), much attention is given to this problem by NHTSA [2]. The reason is that this type of rollover is caused by vehicle-related factors and, therefore, can be prevented by better vehicle safety standards.

The causes of on-road untripped rollover are not well understood; however, some literature shows that it can occur due to both roll and yaw instability [3]. Roll instability may cause a vehicle to rollover during critical manoeuvre such as 'J-turn' manoeuvre at high speeds. Substantial research has been conducted on transient roll analysis, and different metrics have been proposed to measure roll stability of the vehicle [4,5]. On the other hand, in certain movements such as 'sine' shape manoeuvre, the vehicle experiences yaw instability that follows by the rollover [3]. Thus, yaw stability in plane motion, referred to as lateral stability in the literature, is another important factor in vehicle dynamics since it has a strong influence on the overall

*Corresponding author. Email: cwu@cc.umanitoba.ca

vehicle safety. In fact, by improving the lateral stability of the vehicle, it is possible to reduce the risk that a driver loses the control of the vehicle [6].

The lateral stability analysis can be carried out using both linear and nonlinear vehicle models. There is a limitation on the information provided by linear models since these models are only valid in the case of manoeuvre with small levels of the lateral acceleration. In the case of high-g manoeuvre, the tyre force saturates, and the linear model is not valid anymore [7]. Therefore, for more reliable information, the nonlinearity of tyres must be considered, and the vehicle model must be analysed as a nonlinear system. Much of the work done in the vehicle stability analysis and control design areas considers a simple nonlinear vehicle model. The main advantage of such a model is the clear relation among vehicle states. In general, for lateral stability analysis, the well-known 'bicycle' vehicle model is adequate. Such a simple nonlinear model makes it possible to follow the effects of the vehicle states and parameters on the overall vehicle dynamics [6].

Stability analysis can be categorised in two groups: the system stability and the structural stability. In the system stability analysis, the disturbance is imposed to the initial states, and the stability of the solutions of the dynamic systems is discussed. For example, in the case of a vehicle model, the system stability analysis indicates whether the vehicle model returns to its stable fixed point when its initial states are disturbed. Also, this type of stability analysis can determine the stability region in the state space where the stability of the dynamic system is guaranteed, for example, the ranges of the disturbed states in which the vehicle model is still stable. This type of stability analysis makes it possible to investigate how vehicle model parameters or driving conditions affect the shape and size of the lateral stability region corresponded to the vehicle model. On the other hand, the structural stability analysis investigates the perturbations of the system parameters. It determines in which range of parameters the system stays stable. Applying the structural stability analysis on a vehicle model, one can define the ranges of the vehicle parameters or driving conditions in which the vehicle remains stable.

To study the stability of the nonlinear systems, the most general theory was introduced by Lyapunov in the late nineteenth century. This theory includes two methods: the so-called linearisation method and the direct method [8]. The linearisation method uses linear approximation around the system equilibriums and provides information about system stability as far as system states are close to equilibrium points. The direct method is not limited to local stability investigation. This method instead of explicitly solving the dynamic system of equations determines the stability based on shrinking of a constructed scalar 'energy-like' function known as a Lyapunov function [8]. However, the difficulties in finding a Lyapunov function for complex systems is the main restriction to apply this powerful method for stability analysis.

In nonlinear stability analysis, the determination of the state-space stability region is the key factor. A vehicle model as a nonlinear system has its own stability region that its size and shape are indicators of vehicle stability during critical manoeuvres [9]. If the states of a vehicle during critical manoeuvre still remains in the stable region, it will move towards a stable equilibrium point along the specific trajectory. A few studies to estimate the lateral stability region of a vehicle have been conducted in the literature. Methods applied in these studies can be generally divided into two groups: Lyapunov-function-based methods and non-Lyapunov-function-based methods [9]. Most of the existing studies in the non-Lyapunov-function-based methods rely on topological methods, in which the stability region is estimated due to the number of system trajectories derived by numerical integration of the system equations, such as the trajectory reversal method proposed by Genesio *et al.* [10]. Intagaki *et al.* [11], by plotting a large number of trajectories and using an applicable understanding, approximated the stability boundary. Samsundar and Huston [12] applied the trajectory reversal method to estimate the lateral stability region for a (two degrees of freedom (2-DOF)) nonlinear vehicle

model. Ko and Lee [9] proposed an algorithm, including the trajectory reversal technique, to determine a lateral stability region of the 3-DOF nonlinear vehicle for the case of constant vehicle speed. Dependence of trajectory-based methods on appropriate selections of the initial conditions is the most important limitation to apply them in stability analysis. On the other hand, investigation on the stability region based on the Lyapunov-function-based method relies on Lyapunov's direct method. For examples, Johnson and Huston [13] applied this method to the lateral stability analysis of a vehicle in straight-line motion at a constant longitudinal velocity. Samsundar and Huston [12] proposed another quadratic Lyapunov function for the same vehicle model and parameters in [13] and by using the tangency points technique found the largest possible lateral stability region associated with their proposed Lyapunov functions. Sadri and Wu [14] followed the method of Johnson and Huston [13] and found a new Lyapunov function which resulted in a larger lateral stability region for the same vehicle model and parameters used in [12,13].

Applying Lyapunov's direct method to investigate the effects of driving conditions on vehicle stability is extremely challenging since there is no constructive technique to find a Lyapunov function. This technique is also infeasible to demonstrate how the vehicle parameters such as vehicle inertial properties or tyre characteristics affect the lateral vehicle stability. As discussed in [14], main limitations on applying Lyapunov's direct method to estimate the lateral stability region can be summarised as limitations on the vehicle model due to difficulties in finding a Lyapunov function, and dependence of the size and shape of the stability region on the selected Lyapunov functions.

The effects of vehicle parameters and driving conditions on lateral vehicle stability have been discussed in the literature. The fundamental work on this subject has been done by Pacejka [15]. An excellent review of related studies in this topic can also be found in [16]. Shen *et al.* [17] proposed the so-called joint-point locus approach to investigate vehicle system handling. This method geometrically determined the equilibria of the system and then their associated stability properties have been discussed based on system trajectories. Ko and Lee [9] by using their proposed topological approach, which is based on the trajectory reversal technique, found that the variation of the driving conditions such as the vehicle velocity, road friction coefficient, and steering input lead to more significant changes in vehicle yaw lateral stability in comparison with the variation of vehicle parameters such as weight distribution and tyre characteristics. As mentioned earlier, in the trajectory-based method, the system trajectories are solved for certain initial conditions. This means that the system behaviour for other initial conditions is not guaranteed. On the other hand, it is almost infeasible to use Lyapunov's direct method for this kind of stability analysis.

A more reliable technique for the stability analysis of a vehicle model is the concept of Lyapunov exponents. Lyapunov exponents are 'invariant' measures of a dynamic system, that is, independent of the initial conditions [18]. They are defined as the average exponential rates of converging or diverging of nearby orbits in the state space [19,20]. The concept of Lyapunov exponents was first introduced by Lyapunov to study the stability of non-stationary solution of ordinary differential equations [21]. It is a powerful tool to categorise the steady-state behaviour of dynamic systems. The method for calculating the Lyapunov exponents is constructive for any dynamic systems. This constructive nature makes it more advantageous over Lyapunov's direct method. The Lyapunov exponents of a dynamic system can be calculated numerically using either the system mathematical model or a time series. Some methods for calculating Lyapunov exponents based on a mathematical model have already been developed [19,22]. Such methods have been widely used to detect chaotic behaviour of complex dynamic systems. In vehicle dynamics area, Liu *et al.* [23] investigated the chaotic behaviour of the vehicle/driver system by using the concept of Lyapunov exponents. Although Lyapunov exponents have mainly been used for diagnosing chaotic systems, there are studies that used them for the

stability analysis of nonlinear systems. For example, Wu *et al.* [24] proved the system stability of their developed feedback control law for an inverted pendulum system by its Lyapunov exponents. Sekhavat *et al.* [25] analysed the stability of hydraulic actuators with an impact controller using the concept of Lyapunov exponents. Some other work in this area has been reviewed in [21]. To the best of the authors' knowledge, this concept has not been applied in vehicle stability analysis yet. However, the previous success of using this concept in other areas [21,24,25] promises its effectiveness in vehicle stability analysis.

This paper proposes to apply the concept of Lyapunov exponents for the system stability and the structural stability analyses of the vehicle model in plane motion. Here, without the loss of generality, a simple nonlinear vehicle model is considered to demonstrate the effectiveness of the concept of Lyapunov exponents in vehicle stability analysis for the first time.

This paper is organised as follows: a brief preliminary on the concept of the Lyapunov exponents for the stability analysis of nonlinear systems is first given in Section 2. In Section 3, the vehicle model for lateral vehicle dynamics is presented. In Section 4, the system stability of the vehicle model is investigated as follows: first, the stability of the vehicle model in straight-line motion is determined. Second, the associated lateral stability region is estimated, and third, the effects of the driving conditions on the lateral stability region are investigated. In Section 5, the structural stability of the vehicle model is addressed by finding the ranges of driving conditions in which the stability of the vehicle is guaranteed. Then, using examples, the largest Lyapunov exponent of the vehicle model is proposed as an indicator to investigate the convergence rate of the disturbed vehicle to its stable fixed point. The conclusion is given in Section 6.

2. Mathematical preliminary

Here, the concept of Lyapunov exponents is briefly reviewed in Section 2.1, followed by the most popular method to calculate all the Lyapunov exponents based on a mathematical model in Section 2.2.

2.1. *Concept of Lyapunov exponents*

The concept of Lyapunov exponents has been introduced to identify the asymptotic behaviour of nonlinear systems. Considering a continuous dynamic system in an n-dimensional state space, this concept monitors the long-term evolution of an infinitesimal n-sphere of initial conditions. Due to the dynamic flow, the n-sphere may deform to an n-ellipsoid as graphically shown in Figure 1 when $n = 2$. The average rates of the length expanding or contracting of the ellipsoid principal axes over an infinite time period are called Lyapunov exponents [19]. The ith one-dimensional Lyapunov exponent, λ_i, can be calculated as

$$\lambda_i = \lim_{t\to\infty} \frac{1}{t} \log_2 \frac{P_i(t)}{P_i(t_0)}, \quad i = 1, 2, \ldots, n, \tag{1}$$

where P_i is the length of the ith ellipsoidal principal axis. Since for each principal axis one Lyapunov exponent can be defined, the total number of system Lyapunov exponents is equal to the dimension of the dynamic system. Although in the calculation of Lyapunov exponents choosing a trajectory (the 'fiducial' trajectory) is needed, the consequence of a theorem of Oseledec [18] proves that Lyapunov exponents are global properties of the dynamic systems and independent of the chosen trajectory ('invariant' measure of the dynamic system). It is

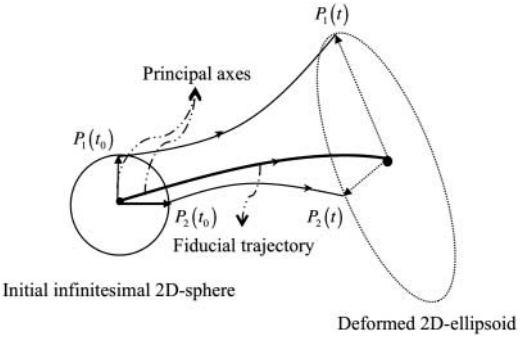

Figure 1. Evolution of infinitesimal two-dimensional sphere of initial conditions (P_i: length of the ith principle axis).

important to note that the orientation of the ellipsoid changes continuously as it evolves. Therefore, it is not possible to define the direction associated with a given exponent.

Both the signs and the values of a system Lyapunov exponent have information about its exponential behaviour. The signs of Lyapunov exponents reveal the stability property of the system's dynamics. Negative exponents correspond to those principal axes of the ellipsoid that shrink in average. If all the exponents are negative, the dynamic system is exponentially stable and the attractor is a fixed point (equilibrium point). Zero exponents indicate the slow change in magnitudes of principal axes. A system with one zero exponent while others are negative has a one-dimensional attractor. For systems with order 3 or more, the positive Lyapunov exponents indicate a chaotic behaviour. In a chaotic system, the long-term behaviour of an initial condition that is specified with any uncertainty cannot be predicted [19]. The sum of all Lyapunov exponents indicates the time averaging divergence of the phase space velocity; hence, for any dissipative dynamic system, the sum of all exponents is negative [19]. This implies that dissipative systems have at least one negative exponent. Moreover, dissipative systems with no fixed point must have at least one zero exponent [26].

In general, there is no feasible analytical way to determine the Lyapunov exponents for a complicated system [27]. Therefore, the Lyapunov exponents are always calculated numerically. They can be calculated using either the system mathematical model or a time series. In practical application, the finite-time Lyapunov exponents are frequently used in the following form:

$$\lambda_i = \frac{1}{t} \log_2 \frac{P_i(t)}{P_i(t_0)}, \quad i = 1, 2, \ldots, n; \tag{2}$$

in the limit as $t \to \infty$, the finite-time Lyapunov exponents converge to the true Lyapunov exponents [28]. In the literature, there are different algorithms to calculate all Lyapunov exponents of a system. The standard algorithm [22] is used in this paper, which will be proceeded in Section 2.2.

2.2. *Calculation of Lyapunov exponents using standard algorithm*

The standard algorithm [22] calculates all Lyapunov exponents of a system defined in the form of a mathematical model. This algorithm starts by selecting an arbitrary initial condition for nonlinear differential equations given in the form of

$$\dot{\boldsymbol{x}} = \boldsymbol{f}(\boldsymbol{x}), \tag{3}$$

where $\boldsymbol{f}$ is an $n \times 1$ nonlinear vector function and $\boldsymbol{x}$ is an $n \times 1$ state vector. The initial n-sphere principal axes are constructed on the selected initial condition. The evolution of the initial condition known as the 'fiducial' trajectory can be found by the action of nonlinear equation (3). To find the evolution of principal axes, another set of equations given in Equation (4) is needed:

$$\dot{\boldsymbol{\psi}}_t = \boldsymbol{F}(t)\boldsymbol{\psi}_t, \tag{4}$$

where $\boldsymbol{\psi}_t$ is called the state transient matrix of the linearised system $\delta\boldsymbol{x}(t) = \boldsymbol{\psi}_t\delta\boldsymbol{x}(0)$ and $\boldsymbol{F}(t)$ is the $n \times n$ Jacobian matrix the elements of which are

$$F_{ij}(t) = \left.\frac{\partial f_i}{\partial x_j}\right|_{x_j = x_j(t)}. \tag{5}$$

To solve Equations (3) and (4) simultaneously, they are represented in one set of equations given as

$$\begin{Bmatrix} \dot{\boldsymbol{x}} \\ \dot{\boldsymbol{\psi}}_t \end{Bmatrix} = \begin{Bmatrix} \boldsymbol{f}(\boldsymbol{x}) \\ \boldsymbol{F}(t)\boldsymbol{\psi}_t \end{Bmatrix}. \tag{6}$$

The standard choice for initial principal axes is orthonormal vectors defined as $\boldsymbol{e}_1(0) = (1, 0, \ldots, 0), \boldsymbol{e}_2(0) = (0, 1, 0, \ldots, 0), \ldots, \boldsymbol{e}_n(0) = (0, \ldots, 0, 1)$. The initial conditions for nonlinear equation (6) are the combination of the selected initial conditions for system of Equations (3) and (4) as given by

$$\begin{Bmatrix} \boldsymbol{x}(0) \\ \boldsymbol{\psi}_t(0) \end{Bmatrix} = \begin{Bmatrix} \boldsymbol{x}_0 \\ \boldsymbol{\psi}_0 \end{Bmatrix}, \tag{7}$$

where the initial state transient matrix is constructed based on initial principal axes as

$$\boldsymbol{\psi}_0 = [\boldsymbol{e}_1^{\mathrm{T}}(0) \cdots \boldsymbol{e}_n^{\mathrm{T}}(0)]_{n\times n}. \tag{8}$$

Integrating the nonlinear equation (6) for initial conditions in Equation (7) for time-step, τ, yields to next set of vectors $\boldsymbol{v}_1(\tau), \boldsymbol{v}_2(\tau), \ldots, \boldsymbol{v}_n(\tau)$. Here, to avoid misalignment of all the vectors along the direction of maximal expansion [19], the Gram–Schmidt reorthonormalisation (GSR) method is applied to orthonormalise these vectors to a new set of principal axes as

$$\begin{aligned} \boldsymbol{e}_1(\tau) &= \frac{\boldsymbol{v}_1(\tau)}{\parallel \boldsymbol{v}_1(\tau) \parallel}, \quad \boldsymbol{e}_2(\tau) = \frac{\boldsymbol{v}_2(\tau) - \langle \boldsymbol{v}_2(\tau), \boldsymbol{e}_1(\tau)\rangle \boldsymbol{e}_1(\tau)}{\parallel \boldsymbol{v}_2(\tau) - \langle \boldsymbol{v}_2(\tau), \boldsymbol{e}_1(\tau)\rangle \boldsymbol{e}_1(\tau) \parallel}, \ldots, \\ \boldsymbol{e}_n(\tau) &= \frac{\boldsymbol{v}_n(\tau) - \langle \boldsymbol{v}_n(\tau), \boldsymbol{e}_1(\tau)\rangle \boldsymbol{e}_1(\tau) - \cdots - \langle \boldsymbol{v}_n(\tau), \boldsymbol{e}_{n-1}(\tau)\rangle \boldsymbol{e}_{n-1}(\tau)}{\parallel \boldsymbol{v}_n(\tau) - \langle \boldsymbol{v}_n(\tau), \boldsymbol{e}_1(\tau)\rangle \boldsymbol{e}_1(\tau) - \cdots - \langle \boldsymbol{v}_n(\tau), \boldsymbol{e}_{n-1}(\tau)\rangle \boldsymbol{e}_{n-1}(\tau) \parallel}. \end{aligned} \tag{9}$$

Figure 2 illustrates the geometrical interpolation of the GSR when $n = 2$. It shows how the $\boldsymbol{v}_1(\tau)$ and $\boldsymbol{v}_2(\tau)$ are orthonormalised to $\boldsymbol{e}_1(\tau)$ and $\boldsymbol{e}_2(\tau)$, respectively. After storing the denominators of $\boldsymbol{e}_1(\tau), \boldsymbol{e}_2(\tau), \ldots, \boldsymbol{e}_n(\tau)$, denoting by $P_1(1), P_2(1), \ldots, P_n(1)$, the nonlinear equation (6) will be integrated for the next time-step τ for new initial conditions already found from the previous step. After storing the denominator of the new principal axes ($P_i(2)$), the integrating process will be repeated. After a large number of integration steps, s, the Lyapunov exponents can be estimated as

$$\lambda_i \approx \frac{\sum_{m=1}^{s} \log_2 P_i(m)}{s\tau} \quad (i = 1, \ldots, n). \tag{10}$$

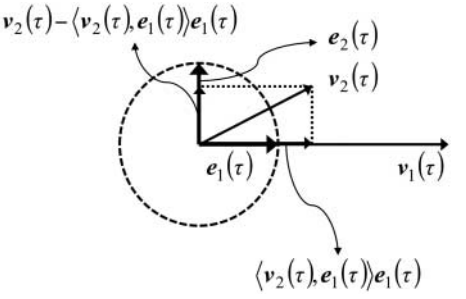

Figure 2. Geometrical interpolation of the GSR method for a two-dimensional system.

The GSR never changes the direction of the first vector in a system; therefore, this vector tends to seek out the most rapidly growing direction in the tangent space [22]. The length of this vector is proportional to $2^{\lambda_1 t}$ for large t. The length of the second vector, which has no component along the direction of the first vector due to the GSR, is proportional to $2^{\lambda_2 t}$ and so on.

3. 2-DOF vehicle model

In this study, the well-known 'bicycle' vehicle model with 2-DOF (the yaw rate and the lateral velocity) and the nonlinear tyre forces is considered. As shown in Figure 3, in this model, the distance between the wheels in front and rear axles is neglected and neither the roll nor the pitch of the vehicle is included. Moreover, the longitudinal velocity, v_x, is assumed to be constant and hence the tractive force equations can be neglected. In a real vehicle, it can be realised by using a cruise control. The (x, y, z) frame (Figure 3) is fixed to the vehicle centre of mass and moves along with the vehicle. The dynamic equations for such a model can be obtained [29,30] as

$$m(\dot{v}_y + v_x r) = F_{yf}\cos\delta_f + F_{yr}, \tag{11}$$

$$I_z\dot{r} = l_f F_{yf}\cos\delta_f - l_r F_{yr}, \tag{12}$$

where m is the total mass of the vehicle, I_z is the vehicle moment of inertia about the z-axis, and l_f and l_r are the distance from the mass centre to the front and rear axles, respectively. F_{yf} and F_{yr} are the tyre lateral forces for the front and rear axles, respectively. δ_f is the front tyre steer angle. v_x is the longitudinal velocity of the vehicle, v_y denotes the lateral velocity of the vehicle, and r stands for the yaw rate of the vehicle around the z-axis.

The following assumptions are made in the vehicle model of this study:

- The vehicle lateral velocity, v_y, and the yaw rate, r, are relatively small in comparison with the vehicle longitudinal velocity, v_x [8]. Thus, the linear relationship among the tyre sideslip angles, lateral velocity, and yaw rate as given in Equations (13) and (14) is valid for front and rear axels, respectively:

$$\alpha_f = \tan^{-1}\left(\frac{v_y + l_f r}{v_x}\right) - \delta_f \approx \frac{v_y + l_f r}{v_x} - \delta_f, \tag{13}$$

$$\alpha_r = \tan^{-1}\left(\frac{v_y - l_r r}{v_x}\right) \approx \frac{v_y - l_r r}{v_x}. \tag{14}$$

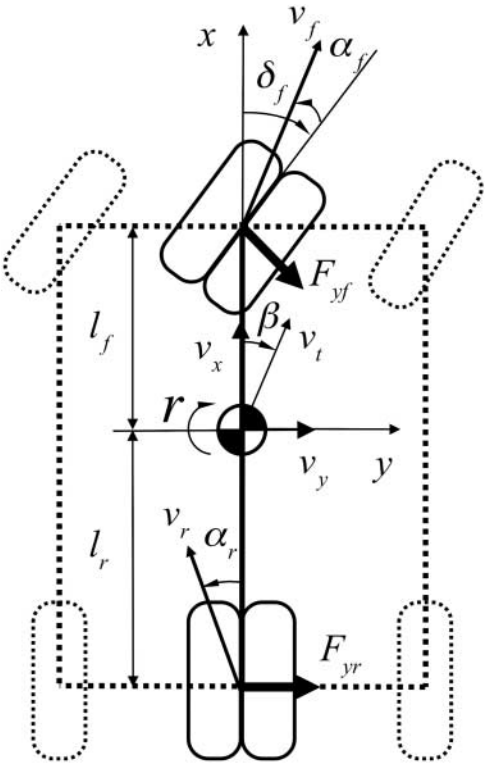

Figure 3. 2-DOF vehicle model.

- The front and the rear sideslip angles, $\alpha_{\rm f}$ and $\alpha_{\rm r}$, are small enough that the nonlinear behaviour of the tyre lateral force can be expressed by the third-order polynomial tyre model [12,13]. Therefore, the tyre lateral force for front and rear axles is related to the corresponded tyre sideslips as given in Equations (15) and (16), respectively:

$$F_{\rm yf} = -2C_{\alpha\rm f}(\alpha_{\rm f} - k_{\rm f}\alpha_{\rm f}^3), \tag{15}$$

$$F_{\rm yr} = -2C_{\alpha\rm r}(\alpha_{\rm r} - k_{\rm r}\alpha_{\rm r}^3), \tag{16}$$

where $k_{\rm f}$ and $k_{\rm r}$ parameters are associated with the nonlinear dependence of the lateral force on the sideslip angle for the front and rear tyres [12,13].

When Equations (13)–(16) are combined with Equations (11) and (12), the nonlinear equations of the vehicle model can be rewritten as

$$\begin{aligned}
\dot{v}_y &= \frac{-2C_{\alpha\rm f}\cos(\delta_{\rm f})((v_y + l_{\rm f}r)/v_x - \delta_{\rm f})[1 + k_{\rm f}((v_y + l_{\rm f}r)/v_x - \delta_{\rm f})^2]}{m} \\
&\quad - \frac{2C_{\alpha\rm r}((v_y - l_{\rm r}r)/v_x)[1 + k_{\rm r}((v_y - l_{\rm r}r)/v_x)^2]}{m} - v_x r, \\
\dot{r} &= \frac{-2C_{\alpha\rm f}l_{\rm f}\cos(\delta_{\rm f})((v_y + l_{\rm f}r)/v_x - \delta_{\rm f})[1 + k_{\rm f}((v_y + l_{\rm f}r)/v_x - \delta_{\rm f})^2]}{I_z} \\
&\quad + \frac{2C_{\alpha\rm r}l_{\rm r}((v_y - l_{\rm r}r)/v_x)[1 + k_{\rm r}((v_y - l_{\rm r}r)/v_x)^2]}{I_z}.
\end{aligned} \tag{17}$$

Table 1. Vehicle model parameters.

Parameters	Values
C_{af}	57,300 N/rad
C_{ar}	57,300 N/rad
k_f	4.87
k_r	4.87
I_z	6550 kg m^2
m	2527 kg
l_f	1.37 m
l_r	1.86 m

This vehicle model is a nonlinear system. The stability properties of the vehicle model governed by Equation (17) with parameter values of a full-size American automobile [12,13], given in Table 1, proceed in the following sections.

4. System stability analysis of the vehicle model

By imposing the disturbance to the initial conditions, the concept of Lyapunov exponents is employed to investigate the system stability of the disturbed vehicle model. In Section 4.1, the stability of the vehicle model in straight-line motion at $v_x = 20$ m/s is discussed. In Section 4.2, the lateral stability region in the phase-plane for the vehicle model in Section 4.1 is estimated. In Section 4.3, the effects of driving conditions such as the longitudinal velocity, road friction coefficient, and steering angle on the lateral stability regions are investigated.

4.1. *Stability analysis of the vehicle model in straight-line motion*

A straight-line motion of the vehicle model can be attained by substituting $\delta_f = 0^\circ$ into Equation (17). It can be easily checked that the origin is one equilibrium point for this special case. In straight-line motion, any non-zero steady-state values for yaw rate and lateral velocity are meaningless. Therefore, other possible equilibrium points are neglected and the stability of the equilibrium point located at the origin is discussed. Since the nonlinear equations describing the vehicle model has two states, two Lyapunov exponents exist. For calculating these two Lyapunov exponents, the initial conditions are chosen as $r_0 = 0.1$ rad/s and $v_{y0} = 1$ m/s. Selecting the time-step size $\tau = 0.001$ s and iterating the standard method for 100,000 times, the first exponent converges to -6.616 and the second one converges to -6.661. Here, it is considered that the convergent exponent is achieved if the change in the numerical values of the exponent between the two subsequent steps is within 10^{-3}. The time history of these exponents is illustrated in Figure 4. All negative exponents indicate that the vehicle model is exponentially stable about the origin equilibrium. Figure 5 displays the system trajectory in the phase-plane for the given initial conditions. It shows how the states of the vehicle model converge to the stable fixed point at the origin of the phase-plane. The time evaluations of the system states are also shown in Figure 6. It can be seen that both states approach to zero since the system is stable.

4.2. *Lateral stability region of the vehicle model in straight-line motion*

For all trajectories start from arbitrary initial conditions in the same stability domain, the Lyapunov exponents have the same values [18]. This property makes it possible to estimate

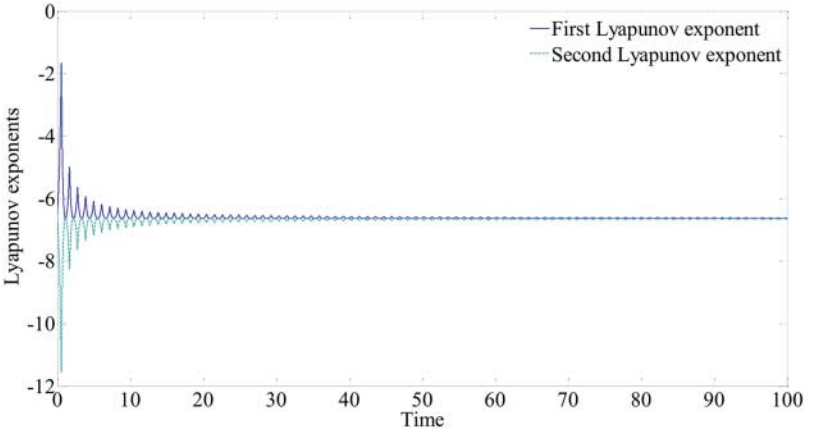

Figure 4. Vehicle model Lyapunov exponents in straight-line motion.

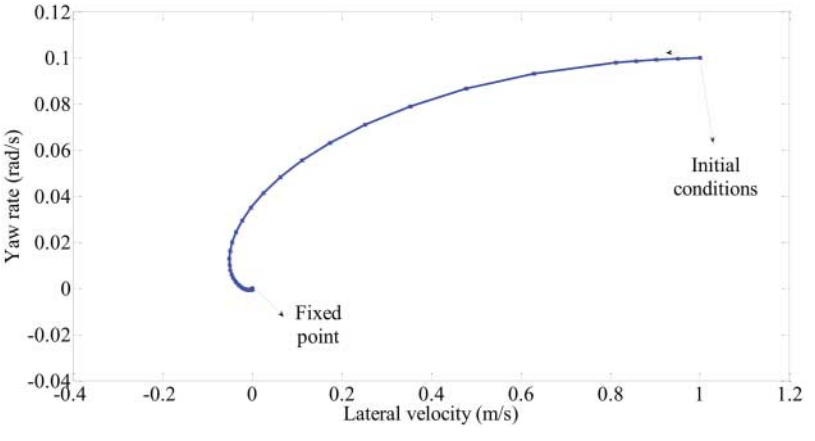

Figure 5. Vehicle model trajectory for initial conditions $r_0 = 0.1\,\mathrm{rad/s}$ and $v_{y0} = 1\,\mathrm{m/s}$.

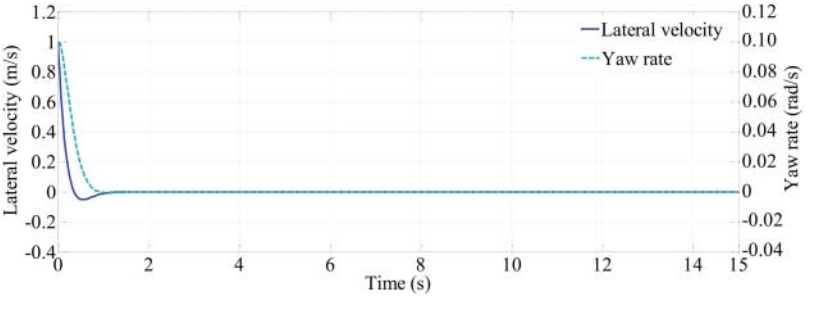

Figure 6. Time evolution of the states of the disturbed vehicle model in straight-line motion.

the stability region. To estimate such a stability region, the $v_y - r$ phase-plane is meshed into small segments. The size of each segment is $0.05\,\mathrm{m/s} \times 0.05\,\mathrm{rad/s}$. Then, the Lyapunov exponents of an arbitrary point in each segment is calculated. The union of those segments which have same negative exponents constructs the lateral stability region [31]. The boundary of the estimated stability region, found by this method, is illustrated by the blue curve in

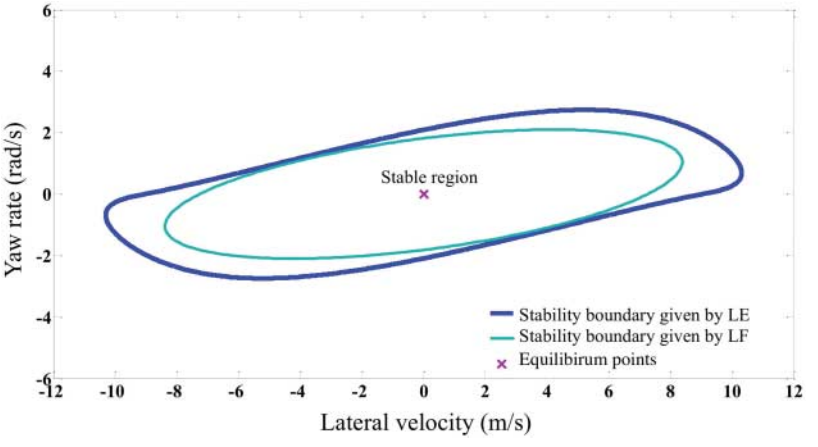

Figure 7. Lateral stability region of the vehicle model in straight-line motion.

Figure 7. For each disturbance inside this border, the vehicle model is exponentially stable and will return to its stable fixed point. The boundary of the lateral stability region given by the proposed Lyapunov function in previous work [14] is also shown by the green curve in Figure 7. This is the largest lateral stability region found by the Lyapunov direct method for this particular vehicle model [12–14]. In the case of Lyapunov's direct method, the size of the stability region is dictated by the specific Lyapunov function, and it is always just the fraction of the overall stability region. For this particular vehicle model, it is quite obvious that the stability boundary extracted by the Lyapunov function is only a portion of the stability region found by the concept of Lyapunov exponents. Here, the lateral stability region, which has been obtained by the concept of Lyapunov exponents, overlaps with the complete lateral stability region found by the simulation in [13]. For each initial condition outside of this area, the calculation of Lyapunov exponents failed since the solution of the equations approaches to infinity. This is the interpretation of the fact that for disturbances outside of this region, the assumption of the constant longitudinal velocity cannot be satisfied even with full throttle as discussed in [7].

4.3. *Effects of the driving conditions on the lateral stability region of the vehicle model*

The lateral stability region of the vehicle model can be deformed due to the vehicle characteristics such as weight disturbance and driving conditions. Since the effect of driving conditions on the lateral stability region is significant [9], in this subsection, the effects of these conditions on the lateral stability region are presented separately.

4.3.1. *Effects of the longitudinal velocity on the lateral stability region*

To investigate the effect of the longitudinal velocity on the stability region, the vehicle model in Equation (17) is supposed to be driven on a straight line on a dry road ($\mu = 1$) at different constant longitudinal velocities. The lateral stability regions for different constant velocities are illustrated in Figure 8. The longitudinal velocities between 15 and 50 m/s are marked on the vertical axis, and their associated lateral stability regions are shown by coloured regions from blue to green. For better demonstration, the projection of the lateral stability regions on planes A, B, and C is also illustrated (Figure 8). As the value of the longitudinal velocity increases, the stability region starts to expand in the lateral velocity direction (see plane C)

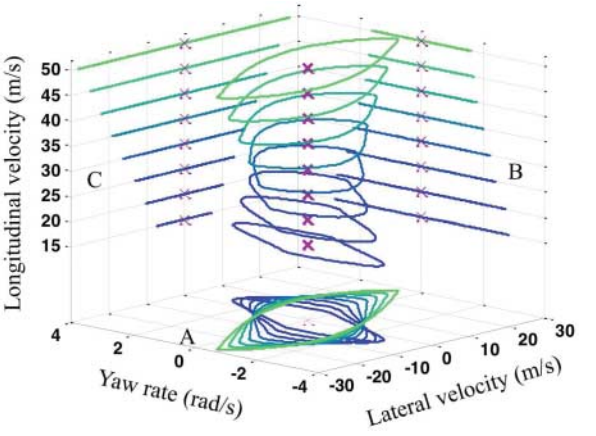

Figure 8. Effects of the longitudinal velocity, v_x, on the lateral stability region.

and to shrink in the direction of the yaw rate (see plane B). These findings are consistent with the previous work [12,15]. This means the vehicle model is less robust to the yaw rate if it is driven at a high constant longitudinal velocity. It can also be seen that the value of the longitudinal velocity does not affect the position of the equilibrium point in the phase-plane of the vehicle model.

4.3.2. *Effects of the road friction coefficient on the lateral stability region*

Since the vehicle model moves due to the tractive force between the road and the tyres, the friction coefficient of the ground contact point plays an important role in its lateral stability. The lateral force between the tyres and the road can be formulated as the multiplication of the tyre normal load and the coefficient of friction ($F_y = \mu N$). Therefore, the coefficient of friction has direct relation with tyre lateral force. To investigate how the coefficient of friction can change the lateral stability region, the vehicle model is driven on a straight line at the constant longitudinal velocity ($v_x = 20\,\mathrm{m/s}$) with the friction coefficient in the range of 0.1–1. In Figure 9, the lateral stability regions associated with different road friction coefficients, shown in the vertical direction, are depicted. The colour changes from blue to green as the road friction increases. The effects of the friction coefficient on lateral stability regions in the direction of the yaw rate and lateral velocity are shown by projections of the lateral stability regions on planes B and C, respectively. It can be found that the stability region mostly shrinks in the direction of the yaw rate (see plane B) due to the decrease in the friction coefficient. On the other hand, the lateral stability region seems to be insensitive in the direction of the lateral velocity by the changes in the friction coefficient (see plane C). It can also be observed that like the longitudinal velocity case, the coefficient of friction does not change the location of the stable equilibrium point on the vehicle model phase-plane.

4.3.3. *Effects of the steering angle on the lateral stability region*

In this case, the vehicle model is driven at the constant longitudinal velocity ($v_x = 20\,\mathrm{m/s}$) around dry circular tracks ($\mu = 1$) with different curvatures. Since the vehicle model moves on a curve, at the steady-state condition, the lateral velocity and yaw rate are non-zero. Therefore, unlike the two other driving conditions, the steering angle input changes the position of the equilibrium point on the phase-plane. In Figure 10, the lateral stability regions for positive

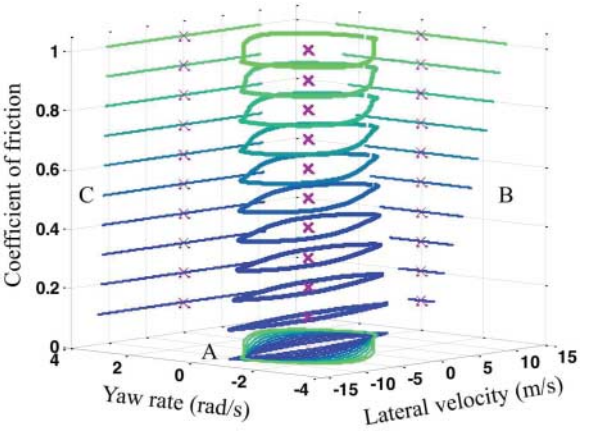

Figure 9. Effects of the friction coefficient between tyres and ground, μ, on the lateral stability region.

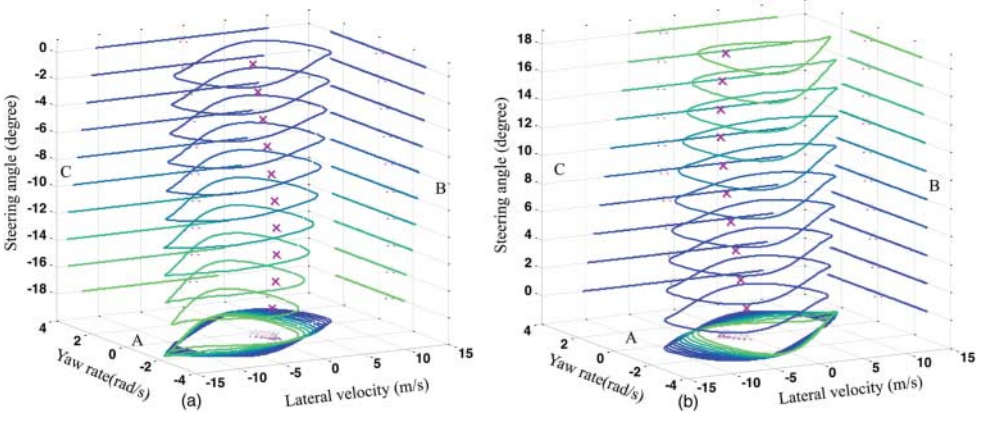

Figure 10. Effects of the steering angle, δ_f, on the stability region: (a) negative steer angles and (b) positive steer angles.

and negative steering angles, indicated on the vertical axis, are shown. For better illustration, the projections of these lateral stability regions on planes A, B, and C are also demonstrated. It can be realised (see planes B and C) that the lateral stability regions start to shrink as the steering angle becomes larger. Furthermore, the stable equilibrium point moves to the boundary (see planes B and C) as the value of the steering angle increases. It means that the vehicle model is generally less robust to the disturbance when it is driven on a sharp circular path.

5. Structural stability analysis of the vehicle model

Structural stability is another important property of a dynamic system. In this section, the above driving conditions are treated as system parameters and are disturbed. The stability region associated with the vehicle model parameters is given in Section 5.1. Section 5.2 deals with the largest Lyapunov exponent of the vehicle model to investigate the convergence rate of the disturbed vehicle model to its stable condition.

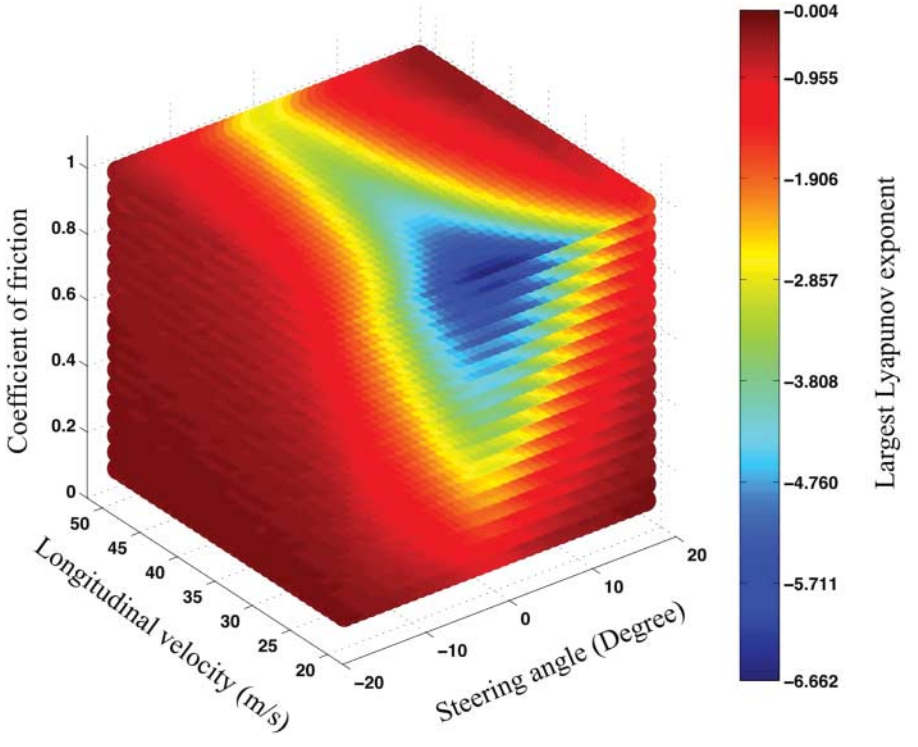

Figure 11. Stability region of the vehicle model.

5.1. *Stability region of the vehicle model*

The stability region gives the ranges of the system parameters in which the stability of the vehicle model is guaranteed. As long as the largest Lyapunov exponent is negative, the system is exponentially stable. Therefore, the sign of the largest Lyapunov exponent is the key to investigate the structural stability of a system.

To find the ranges of the driving conditions in which the stability of the vehicle model is guaranteed, the largest Lyapunov exponent for different vehicle parameters is calculated. Figure 11 shows part of the stability region. Here, it is supposed that the steering angle, longitudinal velocity, and road friction coefficient vary from -18° to 18°, 15 to 50 m/s, and 1 to 0.1, respectively. The step sizes are equal to 0.5° for the steering angle, 1 m/s for the longitudinal velocity, and -0.05 for the coefficient of friction. From Figure 11, it can be found that if the vehicle is driven in conditions belonging to this stability region, the largest Lyapunov exponent is negative and the vehicle model is exponentially stable. The colour map in Figure 11 shows how the absolute value of the largest Lyapunov exponents decreases as the driving conditions approach to the edges. Figure 11 only shows part of the stability region. Determining the entire stability region is important, but beyond the scope of this work.

5.2. *Largest Lyapunov exponent as convergence rate of the disturbed vehicle model to its stable fixed point*

The sum of the Lyapunov exponents indicates the time-averaged divergence of the phase space velocity for a dynamic system [19]. Thus, the value of the largest Lyapunov exponent for a dynamic system with all negative Lyapunov exponents is a qualitative measurement for

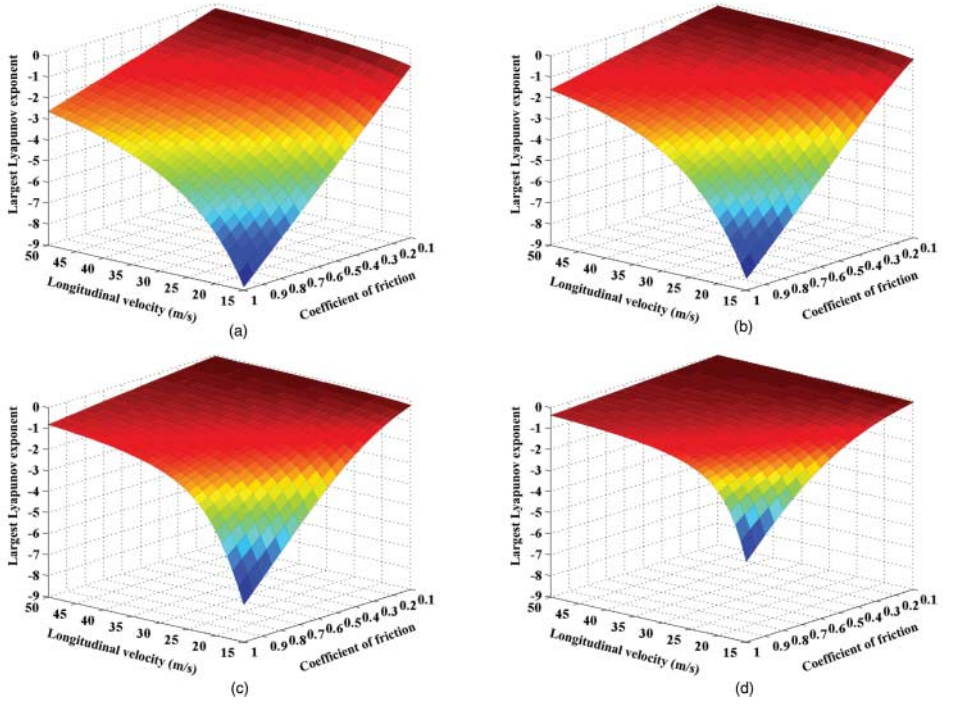

Figure 12. Ranges of longitudinal velocities, v_x, and friction coefficients, μ, in which the stability of the vehicle model is guaranteed while the steering angle, δ_f, is equal to (a) $\delta_f = 0°$, (b) $\delta_f = \pm 5°$, (c) $\delta_f = \pm 10°$, and (d) $\delta_f = \pm 15°$.

the convergence rate in which the disturbed system returns to its stable fixed point in the phase-plane. In this section, this idea is investigated for the vehicle model.

5.2.1. *Example 1: Disturbed vehicle model convergence rate to its stable fixed point for particular steering angles*

In the first example, for a particular value of the steering angle, the largest Lyapunov exponents of the vehicle model with different longitudinal velocities and road friction coefficients are calculated. Figure 12 illustrates the bifurcation diagram of the largest Lyapunov exponent for the steering angle equal to (a) $\delta_f = 0°$, (b) $\delta_f = \pm 5°$, (c) $\delta_f = \pm 10°$, and (d) $\delta_f = \pm 15°$. Here, the longitudinal velocity is in the range of 15–50 m/s with an increment of 1 m/s at each step. The coefficient of friction starts from 0.1, increments 0.05 until it reaches the maximum value of 1. Comparing Figure 12(a) with 12(d), it can be seen that for a particular pair of the longitudinal velocity and the coefficient of friction, for example, $v_x = 15$ m/s and $\mu = 1$, as the steering angle increases, the absolute value of the largest Lyapunov exponent becomes smaller and, therefore, the convergence rate to the stable fixed point in the phase-plane will decrease.

5.2.2. *Example 2: Disturbed vehicle model convergence rate to its stable fixed point for particular longitudinal velocities*

In this example, for particular values of the longitudinal velocity equal to (a) $v_x = 20$ m/s, (b) $v_x = 30$ m/s, (c) $v_x = 40$ m/s, and (d) $v_x = 50$ m/s as shown in Figure 13, the largest Lyapunov exponents of the vehicle model for different steering angles and road friction coefficients are

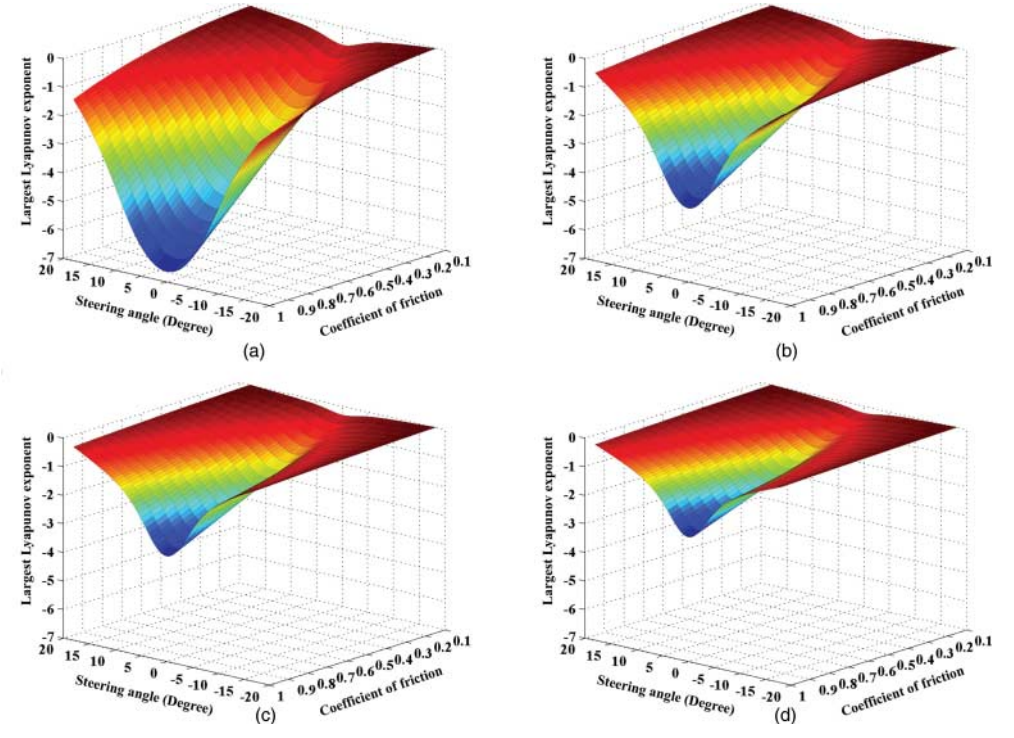

Figure 13. Ranges of steering angles, δ_f, and friction coefficients, μ, in which the stability of the vehicle model is guaranteed while the longitudinal velocity, v_x, is equal to (a) $v_x = 20\,\mathrm{m/s}$, (b) $v_x = 30\,\mathrm{m/s}$, (c) $v_x = 40\,\mathrm{m/s}$, and (d) $v_x = 50\,\mathrm{m/s}$.

calculated. In this figure, the friction coefficient is changed from 0.1 to 1 with the step size equal to 0.05, and the steering angle is changed from $-18°$ to $18°$ with the step size equal to $0.5°$. Each Figure 13(a)–(d) separately shows how the largest Lyapunov exponent varies as the steering angle or/and road friction coefficient changes. Comparing Figure 13(a) with 13(d), it can be realised that for the same steering angle and the road friction coefficient, the disturbed vehicle model has lower convergence rate to its stable fixed point when it is driven at a higher longitudinal velocity.

5.2.3. *Example 3: Disturbed vehicle model convergence rate to its stable fixed point for particular road friction coefficients*

To investigate the effects of the steering angle and the longitudinal velocity on the convergence rate, it is assumed that the vehicle model is driven on the road with different coefficients of friction as (a) $\mu = 1$, (b) $\mu = 0.7$, (c) $\mu = 0.5$, and (d) $\mu = 0.3$. In Figure 14, the maps of largest Lyapunov exponents in these conditions are depicted. In this figure, the steering angle and the longitudinal velocity vary from $-18°$ to $18°$ and 15 to $50\,\mathrm{m/s}$, respectively. The step size associated with the steering angle is equal $0.5°$ and with the longitudinal velocity is $1\,\mathrm{m/s}$. It can be found that in each condition as the steering angle increases or longitudinal velocity increases, the absolute value of the largest Lyapunov exponents decreases and, therefore, the convergence rate of the disturbed vehicle model to return to its stable fixed point will decrease. The comparison among Figure 14(a)–(d) shows that for the same conditions of the steering angle and longitudinal velocity of the vehicle model, the absolute value of the largest Lyapunov exponent becomes smaller as the coefficient of the friction decreases. This can be interpreted

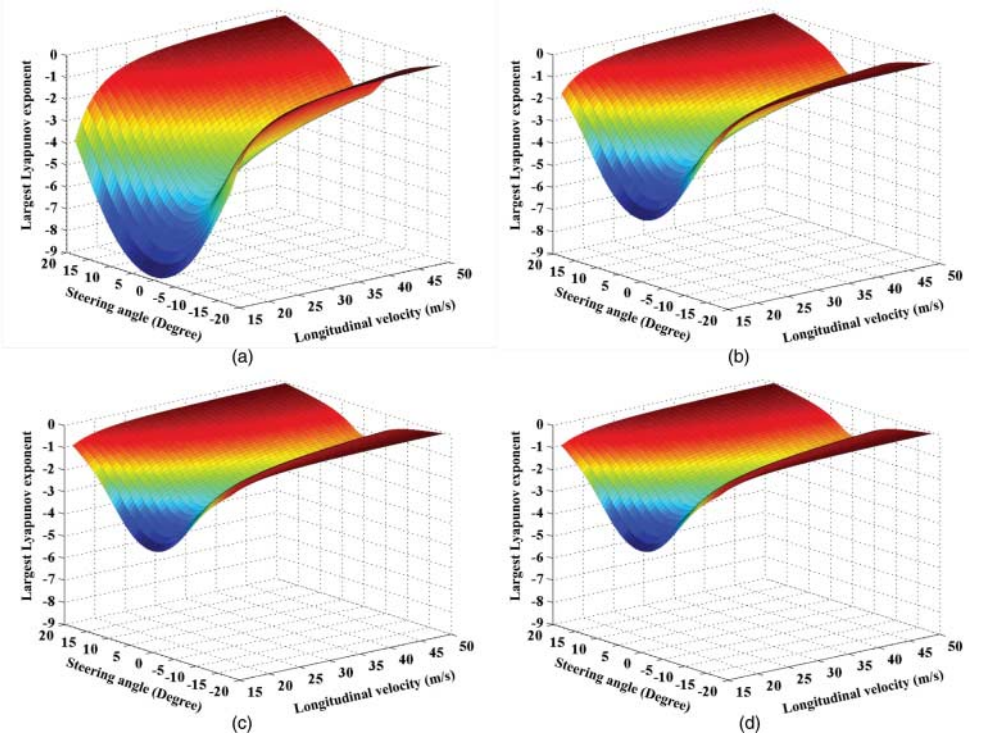

Figure 14. Ranges of steering angles, δ_f, and longitudinal velocity, v_x, in which the stability of the vehicle model is guaranteed while the coefficient of friction, μ, is equal to: (a) $\mu = 1$, (b) $\mu = 0.7$, (c) $\mu = 0.5$, and (d) $\mu = 0.3$.

as the lower convergence rate of the disturbed vehicle model in more slippery roads while the steering angle and longitudinal velocity are the same.

6. Conclusions

This paper has proposed to use the concept of Lyapunov exponents to the lateral stability analysis of a vehicle model. This concept is a powerful tool for stability analysis since the calculation of Lyapunov exponents is constructive for general dynamic systems. Moreover, the Lyapunov exponents are an 'invariant' measure of the dynamic systems, that is, the Lyapunov exponents are independent of initial conditions. For the first time in the vehicle area, this concept has been applied to both system and structural stability analyses of a nonlinear 2-DOF vehicle model.

In system stability analysis, (a) the stability of the vehicle model in straight-line motion is investigated. (b) The lateral stability region of the vehicle model in the case of straight-line motion has been estimated. It has been shown that in this special case, the estimated lateral stability region was the largest one in comparison with those found by Lyapunov's direct method [12–14]. (c) The effects of driving conditions on lateral stability regions of the vehicle model have been discussed. All results were in agreement with those in [9], which verifies the successful application of this concept in vehicle stability analysis.

In the case of structural stability analysis, the ranges of driving conditions in which the vehicle model stability is guaranteed have been found. Moreover, it has been shown that for a disturbed vehicle model, the largest Lyapunov exponent varies for different driving conditions.

Therefore, the largest Lyapunov exponent can be used to investigate how fast the disturbed vehicle model in different driving conditions will return to its stable fixed point.

Although the vehicle model considered in this study is over-simplified, the goal was to demonstrate the power of the concept of Lyapunov exponents to the analysis of vehicle lateral stability. Such an analysis is crucial to keep vehicle safety and there is a pressing need for developing a constructive and theoretically sound approach to vehicle stability analysis. Existing methods are either not constructive, such as Lyapunov-function-based methods, or sensitive to the individual testing or initial conditions, such as simulation-based methods. The proposed method based on the concept of Lyapunov exponents is constructive and theoretically sound, since the exponents are an 'invariant' measure of system dynamics. Furthermore, it has been demonstrated that the proposed method is effective for analysing both the system stability and the structural stability.

As discussed earlier, the presented method for calculating Lyapunov exponents is applicable to general dynamic systems provided that the mathematical models are available. Therefore, the proposed method can be extended to more realistic vehicle models, especially those with roll motion, which is the subject of future work.

Acknowledgement

We acknowledge the funding from Natural Sciences and Engineering Research Council of Canada.

References

[1] National Highway Traffic Safety Administration, *Initiative to address the mitigation of vehicle rollover*, Docket No. NHTSA-2003-14622-1, 2003.
[2] G.J. Forkenbrock and W.R. Garrott, *Vehicle Dynamic Rollover Propensity*, National Highway Traffic Safety Administration. Available at http://www.nhtsa.gov/Research/Vehicle+Dynamic+Rollover+Propensity/ (accessed July 31, 2012).
[3] N. Zhang, G.M. Dong, and H.P. Du, *Investigation into untripped rollover of light vehicles in the modified fishhook and the sine maneuvers. Part I: Vehicle modeling, roll and yaw instability*, Veh. Syst. Dyn. 46(4) (2008), pp. 271–293.
[4] S.C. Peters and K. Lagnemma, *Stability measurement of high speed vehicles*, Veh. Syst. Dyn. 47(6) (2009), pp. 701–720.
[5] S. Lapapong and S.N. Brennan, *Terrain-aware rollover prediction for ground vehicles using the zero-moment point method*, American Control Conference, Baltimore, MD, 2010.
[6] Y.E. Ko and C.K. Song, *Vehicle modeling with nonlinear tires for vehicle stability analysis*, Int. J. Automot. Technol. 11(3) (2010), pp. 339–344.
[7] J. Hernandez and C.Y. Kuo, *Lateral control of higher order nonlinear vehicle model in emergency maneuvers using absolute positioning GPS and magnetic markers*, IEEE Trans. Veh. Technol. 53(2) (2004), pp. 372–384.
[8] J.J.E. Slotine and W. Li, *Applied Nonlinear Control*, Prentice Hall International Inc., Upper Saddle River, NJ, 1991.
[9] Y.E. Ko and J.M. Lee, *Estimation of the stability region of a vehicle in plane motion using a topological approach*, Int. J. Veh. Des. 30(3) (2002), pp. 181–192.
[10] R. Genesio, M. Tartaglia, and A. Vicino, *On the estimation of asymptotic stability regions: State of the art and new proposals*, IEEE Trans. Autom. Control 30(8) (1984), pp. 747–755.
[11] S. Inagaki, I. Kshiro, and M. Yamamoto, *Analysis on vehicle stability in critical cornering using phase-plane method*, International Symposium on Advanced Vehicle Control, Tsukuba-shi, 1994.
[12] J. Samsundar and J.C. Huston, *Estimating lateral stability region of a non-linear 2 degree-of-freedom vehicle*, SAE Technical Paper 981172, 1998, pp. 1791–1797.
[13] D.B. Johnson and J.C. Huston, *Nonlinear lateral stability analysis of road vehicles using Lyapunov's second method*, SAE Technical Paper 841057, 1984, pp. 798–805.
[14] S. Sadri and Q. Wu, *Lateral stability analysis of on-road vehicles using Lyapunov's direct method*, IEEE Intelligent Vehicles Symposium, Alcala de Henares, 2012.
[15] H.B. Pacejka, *Tire and Vehicle Dynamics*, Published on behalf of Society of Automotive Engineering, Warrendale, PA, 2002.
[16] G.M. Dong, N. Zhang, and H.P. Du, *Investigation into untripped rollover of light vehicles in the modified fishhook and the sine maneuvers, part II: Effect of vehicle inertia property, suspension and tyre characteristics*, Veh. Syst. Dyn. 49(6) (2011), pp. 949–968.

[17] S. Shen, J. Wang, P. Shi, and G. Premier, *Nonlinear dynamics and stability analysis of vehicle plane motions*, Veh. Syst. Dyn. 45(1) (2007), pp. 15–35.
[18] V.I. Oseledec, *A multiplicative ergodic theorem: Lyapunov characteristic numbers for dynamical system*, Trans. Moscow Math. Soc. 19 (1968), pp. 197–231.
[19] A. Wolf, J.B. Swif, H.L. Swinney, and J.A. Vastano, *Determining Lyapunov exponents from a time series*, Physica 16D (1985), pp. 285–317.
[20] K.T. Alligood, T.D. Saure, and J.A. Yorke, *Chaos, an Introduction to Dynamical Systems*, Springer, New York, 1997.
[21] C. Yang and Q. Wu, *On stability analysis via Lyapunov exponents calculated from a time series using nonlinear mapping – a case study*, Nonlinear Dyn. 59(1–2) (2010), pp. 239–257.
[22] K. Ramasubramanian and M.S. Sriram, *A comparative study of computation of Lyapunov spectra with different algorithms*, Phys. D 139(1/2) (2000), pp. 72–86.
[23] Z. Liu, G. Payre, and P. Bourassa, *Nonlinear oscillations and chaotic motions in a road vehicle system with driver steering control*, Nonlinear Dyn. 9(3) (1996), pp. 281–304.
[24] Q. Wu, P. Sekhavat, N. Sepehri, and S. Peles, *On design of continuous Lyapunov's feedback control*, J. Franklin Inst. – Eng. Appl. Math. 342(6) (2005), pp. 702–723.
[25] P. Sekhavat, N. Sepehri, and Q. Wu, *Impact control in hydraulic actuators with friction: Theory and experiments*, J. Int. Fed. Autom. Control 14(12) (2006), pp. 1423–1433.
[26] H. Haken, *At least one Lyapunov exponent vanishes if the trajectory of an attractor dose not contain a fixed point*, Phys. Lett. A 94(2) (1983), pp. 71–72.
[27] M. Kunze, *Non-smooth Dynamical Systems*, Springer, Berlin, 2000.
[28] X. Zeng, R.A. Pielke, and R. Eykholt, *Extracting Lyapunov exponents from short time series of low precision*, Mod. Phys. Lett. B 6 (1992), pp. 55–75.
[29] J.R. Ellis, *Vehicle Dynamics*, Business Books Ltd, London, 1969.
[30] D. Smith and J. Starkey, *Effect of model complexity on the performance of automated vehicle steering controllers: Model development, validation and comparison*, Veh. Syst. Dyn. 24(2) (1995), pp. 163–181.
[31] H. Nusse and J.A. York, *Dynamics: Numerical Exploration*, Springer, New York, 1998.